Available online at www.sciencedirect.com
SCIENCE DIRECT
Applied Catalysis B: Environmental 63 (2006) 178–186
APPLIED CATALYSIS B: ENVIRONMENTAL
www.elsevier.com/locate/apcatb

Gold catalysts supported on mesoporous zirconia for low-temperature water–gas shift reaction

V. Idakiev [a,*], T. Tabakova [a], A. Naydenov [b], Z.-Y. Yuan [c,d], B.-L. Su [c]

[a] *Institute of Catalysis, Bulgarian Academy of Sciences, Acad. G. Bonchev Street, bl. 11, 1113 Sofia, Bulgaria*
[b] *Institute of General and Inorganic Chemistry, Bulgarian Academy of Sciences, Acad. G. Bonchev Street, bl. 11, 1113 Sofia, Bulgaria*
[c] *Laboratory of Inorganic Materials Chemistry, The University of Namur (FUNDP), 61 Rue de Bruxelles, B-5000 Namur, Belgium*
[d] *Department of Materials Chemistry, Nankai University, Tianjin 300071, PR China*

Received 3 July 2005; received in revised form 5 October 2005; accepted 7 October 2005
Available online 4 November 2005

Abstract

Mesoporous ZrO_2 with high surface area and uniform pore size distribution, synthesized by surfactant templating through a neutral $[C_{13}(EO)_6–Zr(OC_3H_7)_4]$ assembly pathway, was used as a support of gold catalysts prepared by deposition–precipitation method. The supports and the catalysts were characterized by powder X-ray diffraction, scanning and transmission electron microscopy, N_2 adsorption analysis, temperature programmed reduction and desorption. The catalytic activity of gold supported on mesoporous zirconia was evaluated in water–gas shift (WGS) reaction at wide temperature range (140–300 °C) and at different space velocities and H_2O/CO ratios. The catalytic behaviour and the reasons for a reversible deactivation of Au/mesoporous zirconia catalysts were studied. The influence of gold content and particle size on the catalytic performance was investigated. The WGS activity of the new Au/mesoporous zirconia catalyst was compared to the reference Au/TiO_2 type A (World Gold Council), revealing significantly higher catalytic activity of Au/mesoporous zirconia catalyst. It is found that the mesoporous zirconia is a very efficient support of gold-based catalyst for the WGS reaction.

Keywords: Gold catalysts; Mesoporous zirconia; Water–gas shift reaction

1. Introduction

The water–gas shift reaction (WGSR) is one of the key steps involved in the automobile exhaust processes, converting CO with water to hydrogen and carbon dioxide and including the produced hydrogen as a very effective reductant for NO_x removal [1]. Furthermore, WGS reaction provides pathway to the production of pure hydrogen that can be employed in fuel-cell power systems. The replacement of the internal combustion engine in cars, motorcycles, tracks, buses, etc. with fuel-cell is a way to provide a realistic solution of environmental protection.

Gold has been regarded as a potentially useful system when it is highly dispersed on a suitable support for various industrial and environmental applications [2]. The state and structure of the support strongly influence the catalytic activity and selectivity of the gold-based catalysts [3–5]. The selection of an efficient support is thus a decisive factor to provide desirable contact between gold and support for good catalytic performance [6].

The nature of supported gold catalysts for the low-temperature WGSR has been a subject of much interest for the last years [7]. High catalytic activity for the WGSR was found for the first time using Au/Fe_2O_3 at low-temperature [8–10]. Gold, supported on well-crystalline titania and zirconia, enables the preparation of highly active catalysts in the studied reaction [11]. It has been established that the gold supported on titanium oxide manifested higher catalytic activity in the WGSR in comparison with other catalysts such as Au/Fe_2O_3, Au/Co_3O_4 [12], $Cu/ZnO/Al_2O_3$, Au/ZnO and Au/Al_2O_3 [13]. Mixed oxide supports (Fe_2O_3–ZnO and Fe_2O_3–ZrO_2), as well as supports of a different crystalline state, e.g. amorphous zirconia and titania, have also been used for gold catalysts in the

* Corresponding author. Tel.: +359 2 9792528; fax: +359 2 9712967.
E-mail address: idakiev@ic.bas.bg (V. Idakiev).

0926-3373/$ – see front matter © 2005 Elsevier B.V. All rights reserved.
doi:10.1016/j.apcatb.2005.10.007

WGSR [11,12,14]. Knell et al. [15] showed that gold catalysts supported on amorphous zirconia exhibit a high initial CO oxidation activity which is due to a synergy between the zirconia and the supported gold particles. The activity decreases significantly over a time scale of ~20 h. Recently, it was found that gold deposited on ceria was very effective in the WGSR [16,17]. However, the relationship between the reducibility of ceria, the structure of the active sites and the reaction mechanism has not been elucidated.

The results obtained for the catalytic activity of different gold catalysts give rise to questions about the effect of the nature of the support, the choice of the preparation method, and the gold particle size on the reducibility of the metal oxide support and certainly on the WGS reaction mechanism. The high surface area and large porosity of the support are well-known to be important for the improvement of catalytic activity and selectivity of the resultant catalysts [18]. In our previous work, mesoporous titania with high surface area and uniform pore size distribution, synthesized via a surfactant templating method, has been found to be a promising support for gold-based catalyst in WGSR [19].

Zirconia is of particular interest due to its large field of applications ranging from catalysis to ceramics [20,21]. The synthesis of ordered mesoporous zirconia with high specific surface area and narrow pore size distribution is of capital importance both from the scientific and industrial application point of view. Recently, a new synthesis protocol of nanostructured mesoporous zirconias was developed through a neutral $[C_{13}(EO)_6–Zr(OC_3H_7)_4]$ assembly pathway, and the understanding on the synthesis mechanism of these mesoporous materials could allow a better control of their textural and structural properties [22]. The synthesized mesoporous ZrO_2 has also been used as a support of gold-based catalysts in complete benzene oxidation, showing high catalytic activity [23].

Herein, we extend the application of mesoporous zirconia as support of gold catalysts in WGSR. We try to shed some light on the relationship between textural and structural characteristics of mesoporous zirconia support, the state of gold particles and the WGS activity of catalyst prepared. The catalytic behaviour and the reasons for deactivation of Au/mesoporous zirconia catalysts are thus studied. The influence of gold content and particle size, space velocity and H_2O/CO ratio on the catalytic performance is investigated. To the best of our knowledge, this is the first time to use mesoporous zirconia supported nanosized gold catalyst in WGSR.

2. Experimental

2.1. Synthesis of mesostructured zirconia support

The mesoporous zirconia was obtained using nonionic surfactant polyoxyethylene(6) tridecylether ($C_{13}(EO)_6$, Aldrich) as templating agent and zirconium *n*-propoxide ($Zr(OC_3H_7)_4$, Chempur) as Zr-source, as previously described [22,23]. The surfactant/zirconia molar ratio was 1.5. The hydrothermal treatment was performed at 80 °C for 24 h. The template was completely removed after 48 h of Soxhlet extraction with ethanol solution. The mesoporous zirconia was dried under vacuum at 80 °C and the support was denoted as Z.

2.2. Preparation of gold-containing catalysts

Different content of gold (2–6 wt.%) was loaded on mesoporous zirconia by deposition–precipitation. A solution of $HAuCl_4·3H_2O$ was used to prepare small particles of supported Au. The gold hydroxide was supported on mesoporous zirconia preliminary suspended in water via the chemical reaction between $HAuCl_4·3H_2O$ and Na_2CO_3 in aqueous solution [19]. The samples were dried under vacuum at 80 °C and calcined in air at 400 °C for 2 h. The catalysts were denoted as 2.5 and 5 AZ for the samples containing different gold loading.

2.3. Sample characterization

The X-ray diffraction (XRD) patterns were obtained with a Philips PW 1820 diffractometer with Cu Kα (1.5418 Å) radiation. Both the continuous and step-scan techniques were used, the latter being employed for quantitative analysis. For the estimation of the average size of gold particles, XRD data were collected in the step-scanning mode in the angle interval of 35–45° (2θ) using steps of 0.02° (2θ) and 10 s per step counting time. The average size of gold particles was determined from XRD line broadening by the Scherrer's equation ($\Phi = K\lambda/\beta \cos\theta$) [24], where Φ is the crystal size, λ the wavelength of the X-ray irradiation, K the usually taken as 0.9 and β is the line width at half-maximum height after subtraction of the instrumental line broadening using silicon as a standard.

The transmission electron micrographs (TEM) were taken using a Philips Tecnai-10 microscope at 100 kV. The sample powders were embedded in an epoxy resin and sectioned with an ultramicrotome, and the sections were then placed on copper grids previously coated by carbon to improve stability and reduce the accumulation of charges.

High-resolution transmission electron microscopy (HRTEM) analysis was performed on a Jeol JEM-2010 microscope at 200 kV. The powdered samples were ultrasonically dispersed in isopropyl alcohol and the obtained suspensions were deposited on a holey carbon film supported a copper grid.

The morphology of the obtained samples was studied by scanning electron microscopy (SEM) on a Philips XL-20 microscope with conventional sample preparation and imaging techniques.

The gold content in catalysts was analyzed by atomic absorption method and made by the Analytical Center of the CNRS, Lyon, France. The measured content of gold loading is shown in Table 1.

Nitrogen adsorption–desorption isotherms were obtained on a Micromeritics TRISTAR 3000 analyzer at −196 °C over a wide relative pressure range from 0.01 to 0.995. The samples

Table 1
Textural properties of the mesoporous zirconia and gold-based catalysts, and the gold contents and particle sizes in the catalysts

Sample	Calcination temperature (°C)	Specific surface area (m^2/g)	Pore diameter (nm)	Pore volume (cm^3/g)[a]	Au content (wt.%)	Au particle size (nm)[b]
Z	80	613	2.1	0.51	–	–
	250	452	1.8	0.33	–	–
	400	142	2.7	0.23	–	–
2.5 AZ	250	286	1.7	0.31	–	–
	400	117	2.6	0.20	2.83	10
5 AZ	250	326	1.8	0.27	–	–
	400	129	2.6	0.16	5.74	7

[a] Total pore volumes at $p/p_0 = 0.99$.
[b] Determined by XRD method.

were degassed under vacuum for several hours before nitrogen adsorption measurements. The pore diameter and the pore size distribution were determined by the Barret–Joyner–Halenda (BJH) method using the adsorption branch of isotherms [25]. The specific surface area was determined by the Brunauer–Emmett–Teller (BET) method [26].

Temperature programmed reduction (TPR) measurements were carried out by a method previously described in Ref. [23] under the following conditions: hydrogen–argon mixture (10% H_2); flow rate 24 ml/min; temperature rise 15 °C/min; sample amount 0.1 g.

Temperature programmed desorption (TPD) of the catalysts was performed in an argon (99.999%) flow with a gas flow rate of 4.4 l/h and a pressure of 0.101 MPa in the temperature range of 20–300 °C with a heating rate of 4 °C/min. The mass of the catalysts was 0.2 g. Maihak (Mod. 710S, NDIR, Germany) gas analyzer was used to identify the CO and CO_2. The CO and CO_2 concentrations were determined with accuracy of ±2 ppm.

2.4. Catalytic activity measurement

Catalytic activity test was performed in a fixed-bed flow reactor at atmospheric pressure and temperature range from 140 to 300 °C. The following conditions were applied: 0.5 cm^3 of catalyst bed volume, 4000 h^{-1} of space velocity, 31.1 kPa of partial pressure of water vapour, and the reactant gas mixture contained 4.494 vol.% CO in argon. The CO and CO_2 content were analyzed on "URAS-3G" and "URAS-2T" (Hartmann & Braun AG) gas analyzers and the catalytic activity was expressed by degree of CO conversion. The activity of catalyst was also studied under either different space velocities or different water vapour partial pressures. The experiments at different water vapour partial pressures were done at a constant flow rate of the CO/Ar mixture.

3. Results and discussion

3.1. Structural and textural characterization

3.1.1. XRD, TEM and SEM analysis

Fig. 1 shows the X-ray diffraction patterns of the mesoporous zirconia as-prepared (Z 80) and calcined at 400 °C (Z 400), and gold-based catalysts calcined at 400 °C with different gold content (2.5 and 5 AZ 400). The X-ray diffractogram of the as-prepared mesoporous zirconia (Z 80) shows only a broad peak located in the 2θ range of 20–40°, indicating that this material is amorphous. After calcination of Z and AZ samples at 400 °C, peaks located at 2θ = 30° (0.30 nm), 34.5° (0.26 nm), 50° (0.18 nm) superimposing on the broad peak, belong to the tetragonal structure of the crystalline zirconia [27], are detected. The X-ray diffraction lines of the support are sharpened with the increase of the calcination temperature, indicating that the crystallization process goes deeper. The typical lines of gold (indicated with *) at 2θ = 38.2° and 44.4° in the gold-containing catalyst samples calcined at 400 °C (2.5 and 5 AZ 400) are seen. The gold lines of catalyst 2.5 AZ 400 are observed more clearly than in the case of 5 AZ 400, while the zirconia diffraction lines of 2.5 AZ 400 have a higher intensity than those of 5 AZ 400. The average particle sizes of gold in 2.5 and 5 AZ 400, calculated by the Scherrer's formula, are 10 and 7 nm, respectively. It is thus suggested that the deposition of gold in higher content could restrain to a certain extent the crystallization of tetragonal ZrO_2 phase and the enlargement of gold particle size, due to the possible interaction between ZrO_2 and gold particles.

Fig. 2 shows the TEM images of the zirconia support and the gold catalyst 2.5 AZ 400. It is obvious that the zirconia material

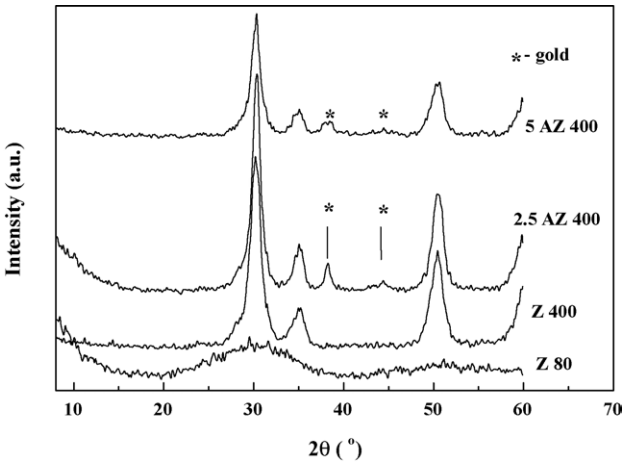

Fig. 1. X-ray diffraction patterns of the mesoporous zirconia as prepared (Z 80) and calcined at 400 °C (Z 400), and gold-based catalysts calcined at 400 °C with different gold content (2.5 and 5 AZ 400). * Indicates the diffraction lines of gold.

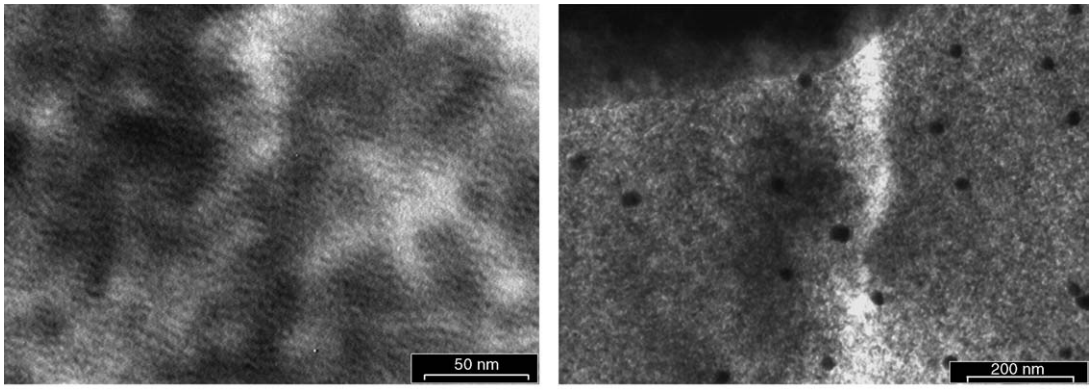

Fig. 2. TEM micrographs of the samples: (a) mesoporous zirconia as-prepared, scale bar 50 nm; (b) gold-based catalyst calcined at 400 °C, scale bar 200 nm.

(Fig. 2a) has a disordered structure with a large number of wormhole-like channels lacking a long-range packing order as reported for DWM [28] or MSU-type materials [29]. Fig. 2b represents an overall view of gold/zirconia sample (2.5 AZ). The gold nanoparticles are relatively homogeneously dispersed with the particle sizes being consistent with that estimated by XRD analysis (Table 1).

The HRTEM analysis performed on 5 AZ reveals that the support is composed of small granular ZrO_2 particles with the sizes from 3.5 to 15 nm (the majority of the nanoparticles are around 6–7 nm in size) (Fig. 3). Some differences on the average size of gold particles estimated by XRD and HRTEM were observed (7 and 13.5 nm, respectively). This is due to the fact that the XRD data are related to coherently scattering domains, whereas HRTEM data are connected to the effective particle dimensions. The supported Au nanoparticles are most probably polycrystalline.

Fig. 4 shows the SEM micrographs, representing the morphologies of the as-prepared and calcined support materials and the gold-based catalysts supported on the mesoporous zirconia. For all of the samples, irregular edge shaped large particles with variable sizes and forms are observed. At the microscopic scale, i.e. micrometer range, the surface of most of samples appears to be very porous. In some case, macropores are detected, which were formed by the aggregation of very small particles. No significant morphological change is noticed after deposition of gold nanoparticles.

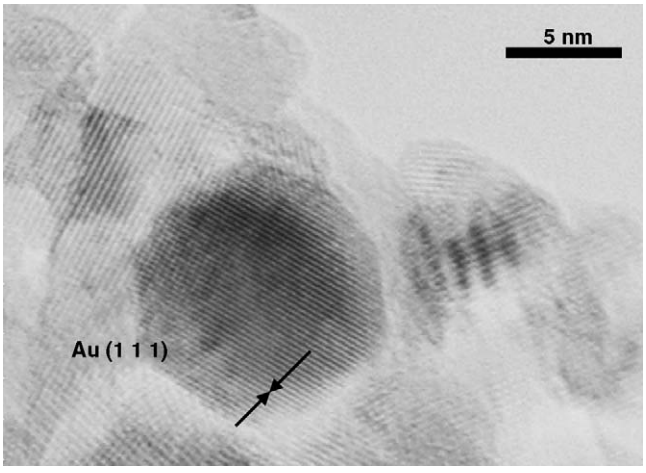

Fig. 3. HRTEM micrograph of gold nanoparticles in the sample 5 AZ 400.

3.1.2. Nitrogen adsorption analysis

The nitrogen adsorption–desorption isotherms and the corresponding pore size distributions of the mesoporous zirconia and gold-based catalysts are depicted in Fig. 5. The isotherms exhibit a linear region from $p/p_0 = 0.1$ to 0.4 before reaching a plateau until a relative pressure p/p_0 equal to 0.85. This kind of isotherm indicates that the present samples belong to the mesoporous family, with pore sizes close to 2.0 nm [30]. For relative pressures superior to 0.90, the adsorbed volume of nitrogen increases significantly instead of remaining constant due to saturation. This means that the samples contain an appreciable amount of secondary mesoporosity or macroporosity as observed on the SEM micrographs. This complementary mesoporosity and macroporosity makes the transport of reagents to framework reaction centers more efficient and thus favors the catalytic activity.

The pore size distributions obtained with BJH method are quite narrow (Fig. 5b), confirming good quality of the samples. The textural properties of the support and catalyst samples are listed in Table 1. It is seen that the surface area of as-prepared mesoporous zirconia decreases from 613 to 142 m^2/g after calcination at 400 °C, while the pore diameter increases from 2.1 to 2.7 nm. After gold loading to be catalysts, the surface areas decrease significantly, as well as the pore volumes. This reduction could be attributed to some insertion of the metallic particles into the mesopores. The shape of the isotherms (Fig. 5a) and the pore sizes did not change significantly (Table 1), meaning that material kept its mesoporous structure after introduction of the metal. The pore diameters of the support and the gold loaded catalysts, both calcined at 400 °C, are practically equal. Interestingly, the surface areas of the catalysts with higher gold loading (5 AZ) are slightly higher than the catalysts with lower gold content (2.5 AZ), whatever the catalysts were calcined at 250 or 400 °C, though the pore volumes of 5 AZ are slight lower than 2.5 AZ. This difference in the surface areas and pore volumes of catalysts with different content of gold loading is in good agreement with the observed

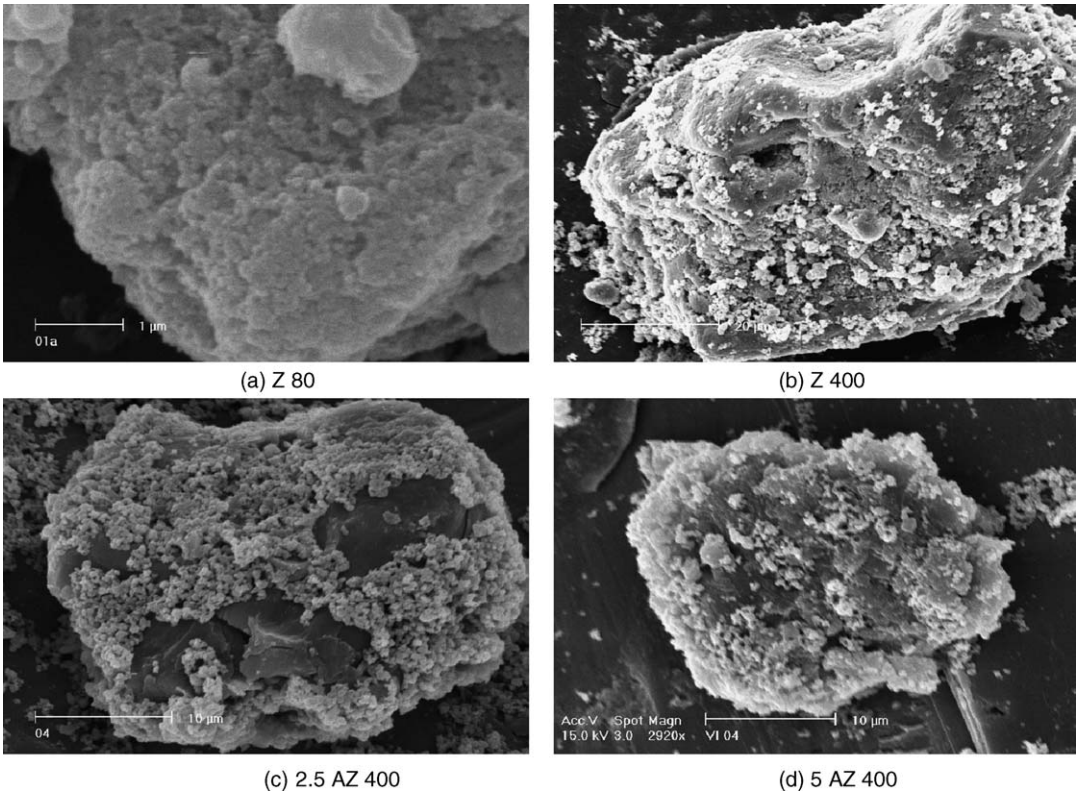

Fig. 4. SEM micrographs of the samples: (a) as-prepared mesoporous zirconia, scale bar 1 μm; (b) mesoporous zirconia calcined at 400 °C, scale bar 20 μm; (c) and (d) gold-based catalysts calcined at 400 °C with different gold content, respectively, scale bar 10 μm.

difference in the crystallinity of the catalyst and support and the gold particle size. The catalysts possessing lower gold loading and larger gold particle size have a lower surface area but with a larger pore volume.

3.1.3. TPR measurements

Fig. 6 depicts the H_2-TPR spectra of the mesoporous zirconia support and its corresponding gold catalyst samples. A significant effect of gold loading on the reducibility of the surface oxygen of mesoporous zirconia is found by H_2-TPR. In the spectrum of mesoporous zirconia calcined at 400 °C (Z 400), no peak is registered till 600 °C, and only a high-temperature (HT) peak is detected at the temperature above 600 °C due to ZrO_2 reduction. Whilst in the spectrum of the catalyst sample of low gold loading content supported on mesoporous zirconia (2.5 AZ 400), two low-temperature (LT) peaks at $T_{max} = 100$ and 210 °C and a broad HT peak at $T_{max} = 550$ °C are detected. The catalyst sample with high gold loading content (5 AZ 400) exhibits a sharp LT peak at $T_{max} = 145$ °C and a shoulder at $T_{max} = 300$ °C, in addition to one HT peak at $T_{max} = 485$ °C. It is clearly seen that the LT peaks shifted to higher temperature with the increase of the content of gold loading, and the HT peaks shifted to the lower temperature. The intensities of the reduction peaks also increase, but the peaks broaden, with the increase of the content of gold loading in the catalyst samples. The LT peaks can be assigned to the reduction of oxygen species on the nanosize gold particles and to the $Zi^{4+} \rightarrow Zi^{3+}$ reduction on the border with gold particles [23]. The shifts of the broad HT peaks to lower temperature and the LT ones to higher temperature can reflect the effect of the gold loading, suggestive of the possible interaction between gold nanoparticles and mesoporous zirconia supports.

3.2. Catalytic activity and stability in WGSR

3.2.1. Catalytic activity

The catalytic activities of the gold catalysts supported on mesoporous zirconia were investigated by the water–gas shift reaction in the temperature range of 140–300 °C. Fig. 7 shows the measured WGSR activities of the samples with different gold content (2.5 and 5 AZ 400), together with the reference catalyst Au/TiO_2 type A (commercially available from World Gold Council). The observed activity of the pure mesoporous zirconia in WGS reaction is imperceptible. It is seen from Fig. 7 that the addition of gold significantly increases the catalytic activity of the samples. The CO conversion observed increases with the content of the gold loading on mesoporous zirconia. The WGS activity of the catalyst 5 AZ 400 is higher than that of the reference Au/TiO_2 type A. These Au/mesoporous zirconia catalysts have even higher WGS activity than the reported Au/mesoporous titania [19].

The higher activity of the sample with higher gold loading (5 AZ) is related to the size of Au particles (7 nm) and the contact structure of Au nanoparticles with the support (Table 1). The role of perimeter interface between Au particles and the support

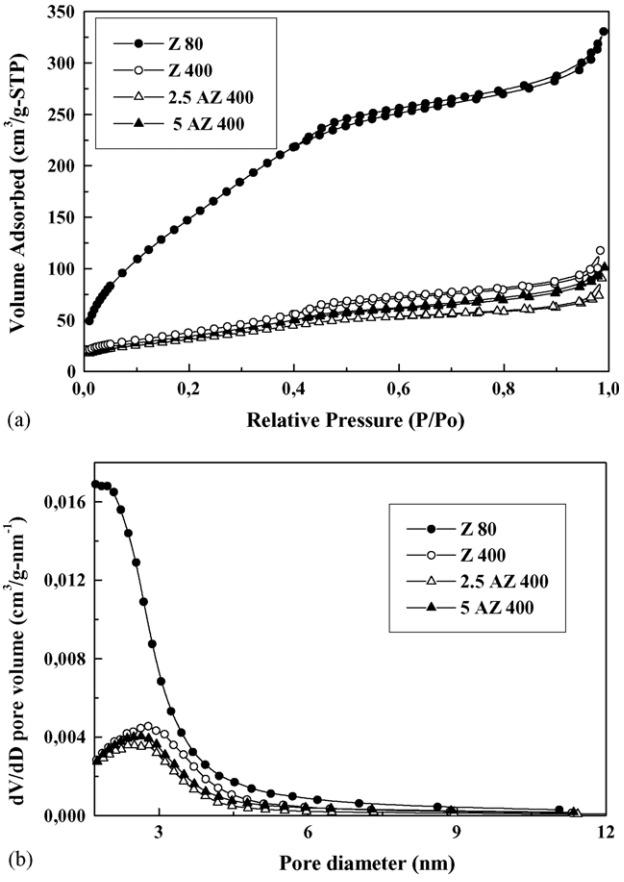

Fig. 5. Nitrogen adsorption isotherms (a) and the corresponding BJH pore size distribution curves (b) of the mesoporous zirconia as-prepared (Z 80) and calcined at 400 °C (Z 400), and gold-based catalysts calcined at 400 °C with different gold content (2.5 and 5 AZ 400).

is emphasized as a unique reaction site for the reactants adsorbed separately, one on Au and another on the support surface [31]. The catalytic activity and selectivity is controlled by the contact structure of Au nanoparticles with the support, the selection of support materials, and the size of Au particles

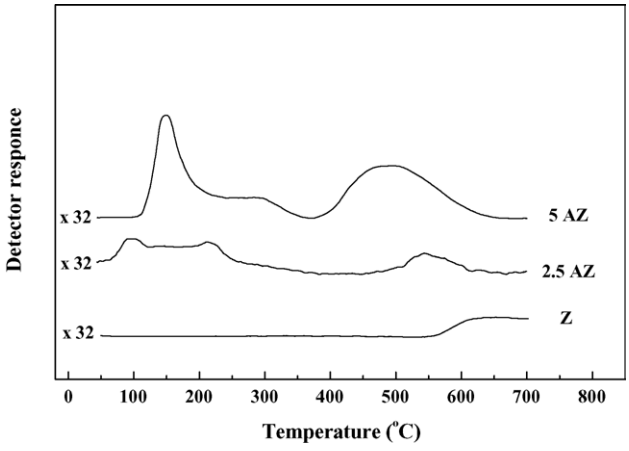

Fig. 6. TPR spectra of the gold-based catalysts and mesoporous zirconia calcined at 400 °C.

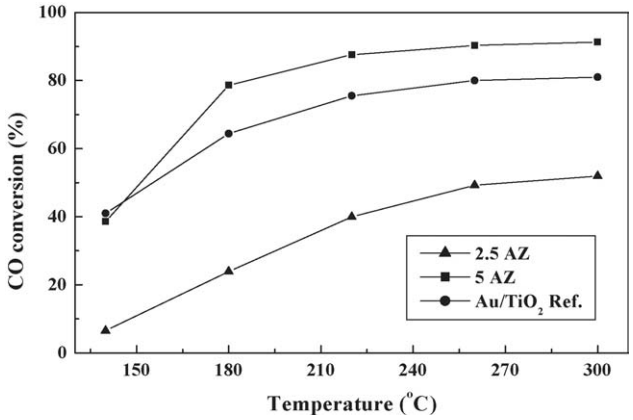

Fig. 7. The WGS activity of the gold/mesoporous zirconia catalysts with different gold content, compared to reference Au/TiO_2 type A from World Gold Council.

[32]. The contact structure is being the most important because the perimeter interfaces around Au particles act as the reaction sites [6]. New reaction sites appear at the metal-support perimeter interface with a decrease in the size of gold particles. When the active sites are edge, corner or step sites, the fractions of the active sites increase when the size of gold particles is smaller [33]. The data in Table 1 show that higher amount of gold (5.74 wt.%) is homogeneously dispersed in the form of hemispherical particles with average size 7 nm on the surface of the 5 AZ catalyst. A smaller amount (2.83 wt.%) of bigger gold particles (10 nm) covers the surface of 2.5 AZ. Moreover the samples 5 AZ possess a higher surface area than 2.5 AZ. It is thus reasonably supposed that the number of active sites located at the Au-support interface of 5 AZ is larger than that of 2.5 AZ. As a result, higher catalytic activity in WGSR is observed in the sample with a higher content of gold loading.

In our previous work of nanosized gold catalyst supported on mesoporous titania that has similar surface area with mesoporous zirconia used herein, the catalyst sample with lower gold loading (2.5 AT) exhibited higher CO conversion than the sample with higher gold content (5 AT) [19]. The sample 2.5 AT possessed smaller gold particle size (4 nm) than

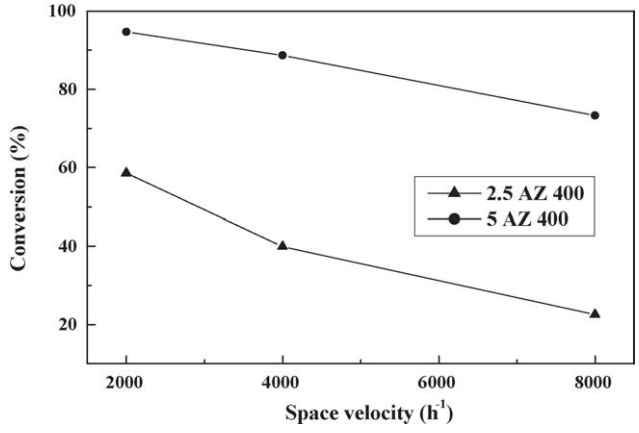

Fig. 8. Effect of contact time on the CO conversion at 220 °C.

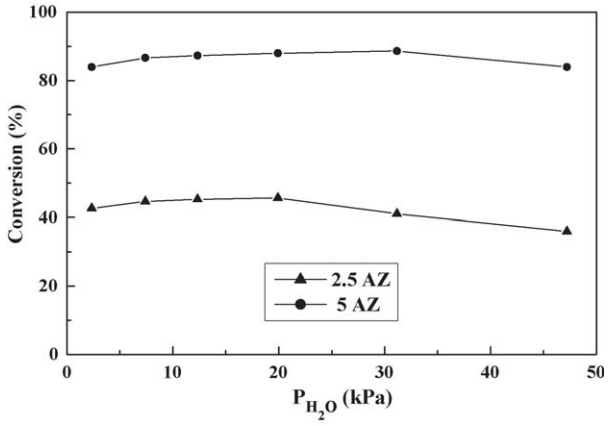

Fig. 9. Effect of H_2O/CO ratio on the CO conversion at 220 °C.

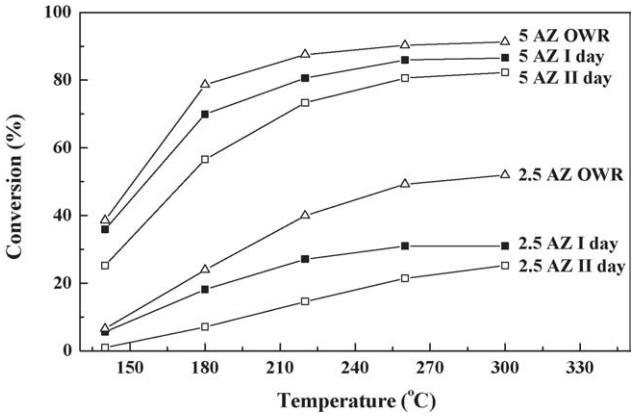

Fig. 10. The WGS activity of the gold catalysts with different content of gold loading before and after regeneration treatment: fresh (2.5 and 5 AZ I day) and reused (2.5 and 5 AZ II day), and after regeneration (2.5 and 5 AZ OWR).

sample 5 AT (6 nm). A comparative analysis of the WGS activities between AZ and AT thus suggests that the activities of the supported gold catalysts correlate with the particle sizes of gold, rather than the content of gold loading, in spite of the different nature of the supports (mesoporous titania and zirconia). The smaller size of the Au particles in the catalysts, the higher activity obtained in WGS reaction. This effect is related to the contact structure between Au nanoparticles and the support.

Fig. 8 presents the effect of contact time on WGS activity at 220 °C over the studied gold/mesoporous zirconia catalysts. The tests were performed with space velocities of 2000, 4000 and 8000 h^{-1}. The sample with higher gold content (5 AZ) demonstrated an insignificant decrease in CO conversion when the space velocity was increased. The effect of contact time on the degree of CO conversion for 2.5 AZ sample is significant.

Fig. 9 illustrates the data for the catalytic activity of the samples at six different H_2O/CO ratios at 220 °C. Very interesting results on the degree of conversion all over the range of investigated water vapour partial pressures were obtained. No serious changes in CO conversion can be seen. The sample with higher gold content (5 AZ) manifests unexpectedly high CO conversion even at rather low H_2O/CO ratios. The catalytic activity very slightly decreases at high H_2O/CO ratios. These results confirm again the high activity of 5 AZ catalyst.

3.2.2. Catalyst stability

One of the most important challenges with nano-gold catalysts is their stability [34,35]. Generally, two reasons for deactivation are under discussion: (i) the agglomeration of gold particles during catalytic test and (ii) the ability of the catalysts to form surface carbonate species. Schubert et al. registered the existence of a carbonate phase formed on the support as a thin surface layer [36]. This carbonate layer on the oxide surface led to the blocking of the active sites. The very recent work of Kim and Thompson also revealed that the deactivation of Au/CeO_2 catalysts in WGSR was due to the formation of carbonates and/or formates on the catalyst surface, which was facilitated by oxygen deficient sites on ceria [37]. The carbonate species appeared to be formed by CO and H_2. However, Zalc et al. attributed the deactivation of Pt/CeO_2 catalysts during WGSR to sintering or over-reduction of the CeO_2 support by H_2 in the reformate [38].

WGS activities of the present catalysts were measured at different temperatures in steady-state conditions after reduction of the samples, and the results are shown in Fig. 10. The fresh catalysts with different gold content were denoted as 2.5 and 5 AZ I day, respectively. After the catalytic test, these catalysts were kept at room temperature in reactant gas mixture for about 12 h, and reused for a second catalytic test (denoted as 2.5 and 5

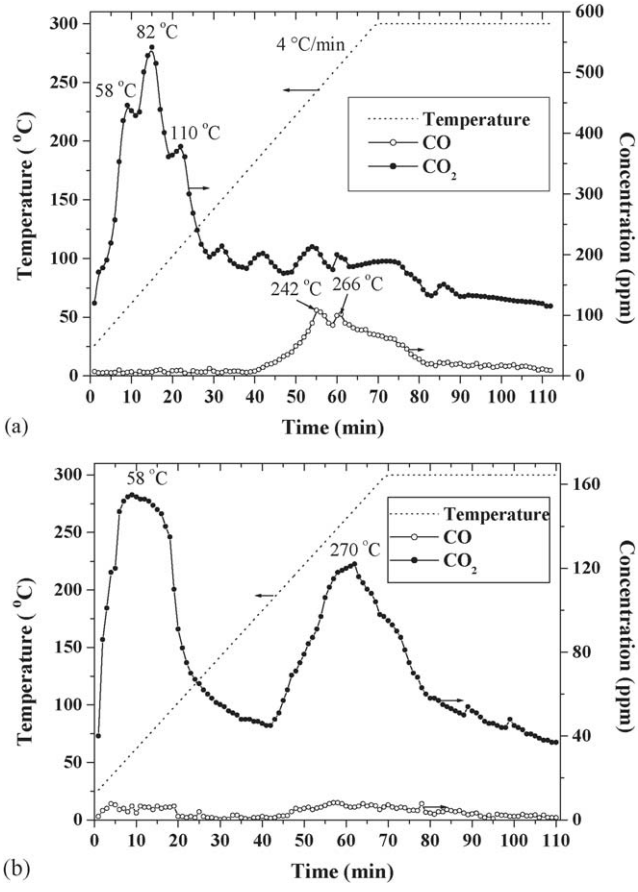

Fig. 11. TPD profiles of the used catalyst samples of (a) 2.5 AZ and (b) 5 AZ.

AZ II day, respectively). The used catalysts were then treated by oxidation for regeneration (denoted as 2.5 and 5 AZ OWR, respectively). As shown in Fig. 10, the catalytic activity decreased significantly in a second catalytic test, in comparison with the first catalytic test. Such a deactivation of Au/mesoporous zirconia seems to be consistent with fouling of the catalyst surface [39], though we are not aware of any reports concerning the deactivation of Au/ZrO_2 catalysts during WGSR.

In order to understand the reason of catalyst deactivation, TPD experiments of the used catalysts were further carried out. The obtained TPD profiles of CO and CO_2 adsorbed in the used 2.5 and 5 AZ samples are presented in Fig. 11. The sample 2.5 AZ exhibits CO desorption peaks around 230–280 °C, and CO_2 desorption peaks around 50–120 °C (Fig. 11a). The total amount of CO and CO_2 detected during temperature-programmed desorption processes are 0.15 and 3.38 mg, respectively. While in the CO–TPD and CO_2–TPD of the catalyst sample with higher gold content (5 AZ), only small amount of CO and CO_2 were detected (0.10 and 1.26 mg, respectively). The CO_2–TPD curve of 5 AZ shows one additional broad peak around 270 °C, besides one desorption peak around 58 °C (Fig. 11b). Comparing with CO_2–TPD profiles, one may believe that CO desorption is quite difficult for the studied catalysts. The results of TPD experiments may be related to the available active sites on the catalyst surface, i.e. larger quantity of desorbed CO and/or CO_2 higher number of available sites on the oxide surface, able to adsorb carbonates.

The catalytic test result of the used catalysts has indicated that deactivation of the supported gold catalysts was inconsistent with earlier reports that the deactivation of reducible oxide-supported noble metal catalysts was due to over-reduction of the support and sintering [38]. Thus the results allow us to deduce that the change in WGS activity of the catalysts is probably due to their tendency to adsorb CO and accumulate it into carbonates. This can be confirmed by the TGA experiments.

Furthermore, if the carbonates deactivate the active sites of the surface, oxidation treatment should regenerate the activity of the catalysts. Indeed, activation with air or air and water vapour at 200 °C for 1 h restored equally the CO conversion, in which H_2O regenerated the active sites by hydrolysis of the carbonate to a bicarbonate and hydroxyl [40]. As shown in Fig. 10, after oxidation treatment of the used catalysts, the activity has been not only recovered, but also higher than the initial one (curves 2.5 and 5 AZ OWR). The lower activity of the fresh catalysts than the regenerated ones may be due to the contaminant adsorption on the sample surfaces before catalytic testing. Anyway, this observation supports the conclusion that deactivation of the Au/mesoporous zirconia catalysts was due to surface fouling and not sintering of the Au or support, or irreversible overreduction of support.

4. Conclusions

Nanosized gold catalysts have been prepared by using mesoporous zirconia of high surface area and uniform pore size distribution as a support, which exhibit high activity in the WGSR. The structure of mesoporous zirconia support facilitates the formation of well-dispersed and stable gold particles on the surface upon calcination and reduction and thus strongly improves the catalytic performances. The different loading content, average particle size and dispersion of the gold strongly influence the catalytic activity. The smaller gold content on mesoporous zirconia leads to the formation of bigger gold nanoparticles and to a significant decrease of the catalytic activity in the water–gas shift reaction. The established slow deactivation of the catalysts is due to their ability to adsorb CO and accumulate it as carbonates. This deactivation is reversible, and the initial activity can be fully restored after heating the deactivated catalysts in air at elevated temperatures.

Acknowledgements

This work was supported by the National Science Fund at the Ministry of Education and Science of Bulgaria (project X-1320), the Joint Research Project between the Commissariat general des relations internationals (CGRI), Belgium and Bulgarian Academy of Sciences, and NATO grant EST.CLG 979797, and the National Basic Research Program of China (grant 2003CB615801). The authors thank Dr. M. Manzoli from Department of Chemistry IFM, University of Torino for providing the HRTEM data.

References

[1] V. Idakiev, Z.Y. Yuan, T. Tabakova, B.L. Su, Appl. Catal. A 281 (2005) 149–155.
[2] G.C. Bond, D.T. Thompson, Catal. Rev. Sci. Eng. 41 (1999) 319–388.
[3] A. Baiker, M. Kilo, M. Maciejewski, S. Menzi, A. Wokaun, in: L. Guczi, F. Salamosi, P. Tetenyi (Eds.), Proceedings of the 10th International Congress on Catalysis, Budapest, 1992, Part B ed., Elsevier Science Publ. B.V., 1993, pp. 1257–1267.
[4] A. Kozlova, S. Sugiyama, A. Kozlov, K. Asakura, Y. Iwasawa, J. Catal. 176 (1998) 426–438.
[5] Y. Yuan, K. Asakura, A. Kozlova, H. Wan, K. Tsai, Y. Iwasawa, Catal. Today 44 (1998) 333–342.
[6] M. Haruta, Cattech 6 (2002) 102–115.
[7] D. Andreeva, Gold Bull. 35 (2002) 82–88.
[8] D. Andreeva, V. Idakiev, T. Tabakova, A. Andreev, J. Catal. 158 (1996) 354–355.
[9] D. Andreeva, V. Idakiev, T. Tabakova, A. Andreev, R. Giovanoli, Appl. Catal. A 134 (1996) 275–283.
[10] D. Andreeva, T. Tabakova, V. Idakiev, P. Christov, R. Giovanoli, Appl. Catal. A 169 (1998) 9–14.
[11] T. Tabakova, V. Idakiev, D. Andreeva, in: L. Petrov, Ch. Bonev, G. Kadinov (Eds.), Proceedings of the 9th International Symposium Heterogeneous Catalysis, 2–27 September, Varna, 2000), pp. 489–494.
[12] D. Andreeva, V. Idakiev, T. Tabakova, R. Giovanoli, Bulg. Chem. Commun. 30 (1998) 59–67.
[13] H. Sakurai, A. Ueda, T. Kobayashi, M. Haruta, Chem. Commun. (1997) 271–272.
[14] T. Tabakova, V. Idakiev, D. Andreeva, I. Mitov, Appl. Catal. A 202 (2000) 91–97.
[15] A. Knell, P. Barnickel, A. Baiker, A. Wokaun, J. Catal. 137 (1992) 306–321.
[16] D. Andreeva, V. Idakiev, T. Tabakova, L. Ilieva, P. Falaras, A. Bourlinos, A. Travlos, Catal. Today 72 (2002) 51–57.
[17] Q. Fu, A. Weber, M. Flytzani-Stephanopoulos, Catal. Lett. 77 (2001) 87.
[18] T.Z. Ren, Z.Y. Yuan, B.L. Su, Chem. Phys. Lett. 388 (2004) 46–49.
[19] V. Idakiev, T. Tabakova, Z.-Y. Yuan, B.-L. Su, Appl. Catal. A 270 (2004) 135–141.

[20] P.D.L. Mercera, J.G. Van Ommen, E.B.M. Doesburg, A.J. Burggraaf, J.R.H. Ross, Appl. Catal. 57 (1990) 127–148.
[21] P.D.L. Mercera, J.G. Van Ommen, E.B.M. Doesburg, A.J. Burggraaf, J.R.H. Ross, Appl. Catal. 71 (1991) 363–391.
[22] J.L. Blin, L. Gigot, A. Leonard, B.L. Su, Stud. Surf. Sci. Catal. 143 (2002) 1035–1043.
[23] V. Idakiev, L. Ilieva, D. Andreeva, J.L. Blin, L. Gigot, B.L. Su, Appl. Catal. A 243 (2003) 25–39.
[24] A. Guiner, X-Ray Diffraction in Crystals, Imperfect Crystals and Amorphous Bodies, Dover Publications, New York, 1994.
[25] E.P. Barret, L.G. Joyner, P.P. Halenda, J. Am. Chem. Soc. 73 (1951) 373–380.
[26] S. Brunauer, P.H. Emmett, E. Teller, J. Am. Chem. Soc. 60 (1938) 309.
[27] F. Del Monte, W. Larsen, J.D. Mackenzie, J. Am. Ceram. Soc. 83 (2000) 1506–1512.
[28] J.L. Blin, A. Leonard, B.L. Su, Chem. Mater. 13 (2001) 3542–3553.
[29] P.T. Tanev, M. Chibwe, T.J. Pinnavaia, Nature 368 (1994) 321–323.
[30] J.L. Blin, A. Léonard, Z.Y. Yuan, L. Gigot, A. Vantomme, A.K. Cheetham, B.L. Su, Angew. Chem. Int. Ed. 42 (2003) 2872–2875.
[31] M. Haruta, M. Date, Appl. Catal. A 222 (2001) 427–437.
[32] M. Haruta, in: Proceedings of the Gold 2003 Conference on New Industrial Applications for Gold, Vancouver, September 28–1 October, 2003.
[33] M. Mavrikakis, P. Stoltze, J.K. Nørskov, Catal. Lett. 64 (2000) 101–106.
[34] P. Konova, A. Naydenov, T. Tabakova, D. Mehandjiev, Catal. Commun. 5 (2004) 537–542.
[35] Ch.H. Kim, L.T. Thompson, in: Proceedings of the Gold 2003 Conference on New Industrial Applications for Gold, Vancouver, September 28–1 October, 2003.
[36] M. Schubert, V. Plzak, J. Garche, R. Behm, Catal. Lett. 76 (2001) 143–150.
[37] C.H. Kim, L.T. Thompson, J. Catal. 230 (2005) 66–74.
[38] J.M. Zalc, V. Sokolovskii, D.G. Löffler, J. Catal. 206 (2002) 169–171.
[39] R. Hughes (Ed.), Deactivation of Catalysts, Academic Press, London, 1984.
[40] M.C. Kung, C.K. Costello, H.H. Kung, Catalysis 17 (2004) 152–165.